

# On the luminosity distance and the epoch of acceleration

Will Sutherland<sup>1\*</sup> and Paul Rothnie<sup>1</sup>

<sup>1</sup>*School of Physics and Astronomy, Queen Mary University of London, Mile End Road, London E1 4NS, UK.*

MNRAS - accepted 2014 Nov 05. Received 2014 Nov 5; in original form 2014 Jun 11

## ABSTRACT

Standard cosmological models based on general relativity (GR) with dark energy predict that the Universe underwent a transition from decelerating to accelerating expansion at a moderate redshift  $z_{\text{acc}} \sim 0.7$ . Clearly, it is of great interest to directly measure this transition in a model-independent way, without the assumption that GR is the correct theory of gravity. We explore to what extent supernova (SN) luminosity distance measurements provide evidence for such a transition: we show that, contrary to intuition, the well-known “turnover” in the SN distance residuals  $\Delta\mu$  relative to an empty (Milne) model does not give firm evidence for such a transition within the redshift range spanned by SN data. The observed turnover in that diagram is predominantly due to the negative curvature in the Milne model, *not* the deceleration predicted by  $\Lambda$  cold dark matter and relatives. We show that there are several advantages in plotting distance residuals against a flat, non-accelerating model ( $w = -1/3$ ), and also remapping the  $z$ -axis to  $u = \ln(1+z)$ ; we outline a number of useful and intuitive properties of this presentation. We conclude that there are significant complementarities between SNe and baryon acoustic oscillations (BAOs): SNe offer high precision at low redshifts and give good constraints on the net *amount* of acceleration since  $z \sim 0.7$ , but are weak at constraining  $z_{\text{acc}}$ ; while radial BAO measurements are probably superior for placing direct constraints on  $z_{\text{acc}}$ .

**Key words:** cosmological parameters – cosmology: observations – dark energy – distance scale.

## 1 INTRODUCTION

The  $\Lambda$  cold dark matter ( $\Lambda$ CDM) model has become well established as the standard model of cosmology, due to its very impressive fit to a variety of cosmological observations, including CMB anisotropy (Hinshaw et al 2013; Planck Collaboration 2014), large-scale galaxy clustering including the baryon acoustic oscillation (BAO) feature (Anderson et al 2014), and the Hubble diagram for distant supernovae (SNe; Betoule et al 2014). In  $\Lambda$ CDM and close relatives, the mass-energy content of the Universe underwent a transition from matter domination to dark energy domination in the recent past at a redshift  $z_{\text{me}} \sim 0.33$ ; the transition from decelerating to accelerating expansion, hereafter  $z_{\text{acc}}$ , was somewhat earlier, at a redshift  $z_{\text{acc}} \approx 0.67$ . In  $\Lambda$ CDM, these are given by  $1+z_{\text{acc}} = \sqrt[3]{2\Omega_{\Lambda}/\Omega_{\text{m}}}$  and  $1+z_{\text{me}} = \sqrt[3]{\Omega_{\Lambda}/\Omega_{\text{m}}}$ , so  $1+z_{\text{acc}} = \sqrt[3]{2}(1+z_{\text{me}})$ . We see later that the value of  $z_{\text{acc}}$  is relatively insensitive to dark energy properties, assuming standard GR and simple parametrizations of the dark energy equation of state.

The most direct evidence for recent accelerated

expansion comes from the many observations of distant SNe at  $0.02 < z \lesssim 1.5$ ; the early SN results in 1998 (Riess et al 1998; Perlmutter et al 1999) began a rapid acceptance of dark energy, due also to previous indirect evidence from large-scale structure (Efsthathiou, Sutherland & Maddox 1990), the cluster baryon fraction (White et al 1993) and the Hubble constant (Ferrarese et al 1996). Strong independent support came from observation of the first CMB acoustic peak defining a near-flat universe (de Bernardis et al 2000; Balbi et al 2000), combined with decisive evidence for a low value of  $\Omega_{\text{m}}$  from the 2dF Galaxy Redshift Survey (Peacock et al 2001; Percival et al 2002). In the past decade there has been a rapid improvement in the precision of observations in all these areas (see references above), most recently from the *Planck*, Baryon Oscillation Spectroscopic Survey (BOSS) and Supernova Legacy Survey (SNLS) projects. Current joint constraints are impressively consistent with  $\Lambda$ CDM with  $\Omega_{\text{m}} \simeq 0.30$  and  $H_0 \simeq 68.3 \text{ km s}^{-1} \text{ Mpc}^{-1}$  (Anderson et al 2014; Betoule et al 2014).

Many deductions in cosmology are based on six, seven or eight-parameter fits of extended  $\Lambda$ CDM to observational data, which generally show good consistency with the six-

\* E-mail: w.j.sutherland@qmul.ac.uk

parameter model and place upper limits on the additional parameters. However, given our substantial ignorance of the nature of dark energy, it is clearly interesting to ask what we can deduce with fewer assumptions, e.g. keeping the cosmological principle while dropping the assumption of standard gravity. In particular, fitting models of GR with dark energy to the data produces a reasonably sharp prediction for the value of  $z_{\text{acc}}$ ; however, if the apparent cosmic acceleration is due to another cause such as modified gravity (Clifton et al 2012), a giant local void (Celerier 2007) or other, this may not necessarily hold; therefore, it is of considerable interest to see what constraints we can place on  $z_{\text{acc}}$  *without* assuming specific models.

It has been shown by e.g. Shapiro & Turner (2006) that the SN brightness/redshift relation does provide evidence for accelerated expansion independent of GR; but direct evidence for past deceleration is less secure. A number of other authors have explored GR-independent constraints on the cosmic expansion history, dark energy evolution and/or  $z_{\text{acc}}$ ; e.g. Sahni & Starobinsky (2006) provide a broad review mainly focused on dark energy reconstruction; Cattoen & Visser (2008) explore various distance definitions related to  $z$  or  $y = z/(1+z)$ ; Cunha & Lima (2008) derived constraints on  $z_{\text{acc}}$  from SNe assuming simple parametrizations of deceleration parameter  $q(z)$ ; Clarkson & Zunckel (2010) provide a method for non-parametric reconstruction of  $w(z)$  (mainly from future high-quality data); Mortsell & Clarkson (2009) provide non-parametric estimates of  $H(z)$ ; and Nesseris & Garcia-Bellido (2013) give a comparison of several methods for estimating  $w(z)$  from SNe data. Our work is partly related to these, but focusing more on the possibility of non-parametric constraints specifically on  $z_{\text{acc}}$ ; where we overlap we are generally in agreement.

The plan of the paper is as follows: in Section 2 we discuss the value of  $z_{\text{acc}}$  and the SN Hubble diagram, and the cause of the downturn in the latter. In Section 3 we point out several advantages of comparing SN residuals relative to a flat non-accelerating model. We discuss some future prospects in Section 4, and we summarize our conclusions in Section 5. Our default model is  $\Lambda$ CDM with  $\Omega_m = 0.300$ ;  $H_0$  generally cancels except where stated.

## 2 RELATION BETWEEN LUMINOSITY DISTANCES AND $z_{\text{acc}}$

### 2.1 The expected value of $z_{\text{acc}}$

Here we note that the value <sup>1</sup> of  $z_{\text{acc}}$  is now constrained rather well in flat  $w$ CDM models with constant dark energy equation of state  $w$ ; for this model family,  $z_{\text{acc}}$  depends on only  $\Omega_m$  and  $w$ , and is given by

$$1 + z_{\text{acc}} = [(-1 - 3w)(1 - \Omega_m)/\Omega_m]^{-1/3w} \quad (1)$$

<sup>1</sup> In highly non-standard models, it is not guaranteed that  $z_{\text{acc}}$  (defined by  $\ddot{a} = 0$ ) is single-valued; e.g. if there were short-period low-amplitude oscillations in  $\dot{a}$ , or a past accelerating phase transitioned back to deceleration at a very low redshift, then in principle  $z_{\text{acc}}$  may be multi-valued. These possibilities appear improbable and hard to test observationally, so we assume  $z_{\text{acc}}$  is single-valued (after the CMB era) for the remainder of this paper; see also Linder (2010).

(e.g. Turner & Riess 2002). This is shown in a contour plot in Fig. 1. It is interesting that in the neighbourhood of  $\Omega_m \sim 0.3$ ,  $w \sim -1$ , the contours of constant  $z_{\text{acc}}$  are nearly vertical, thus  $z_{\text{acc}}$  is nearly independent of  $w$  and is well approximated by

$$z_{\text{acc}} \simeq 0.671 - 2.65(\Omega_m - 0.3) \quad (2)$$

Qualitatively, this occurs because as  $w$  increases above  $-1$ , there is less negative pressure hence less acceleration per unit  $\rho_{DE}$ , but larger  $w$  gives higher  $\rho_{DE}$  in the past; these effects happen to cancel (largely coincidentally) near the concordance model, so  $z_{\text{acc}}$  is rather insensitive to  $w$ . This has positive and negative consequences: on the one hand, measuring  $z_{\text{acc}}$  is not useful for constraining  $w$ ; on the other hand, the range  $0.60 \leq z_{\text{acc}} \leq 0.75$  appears to be a robust prediction of  $w$ CDM, so if future data (e.g. direct measurements of  $H(z)$  from BAOs or cosmic chronometers, or new more precise SN data) were to empirically measure  $z_{\text{acc}}$  *outside* this range, it could essentially falsify the whole class of  $w$ CDM models. (Models with time-varying  $w$  such as the common model  $w(a) = w_0 + w_a(1 - a)$  allow a wider range of  $z_{\text{acc}}$ , but these generally require  $z_{\text{acc}} < 1$  unless  $w_a$  is dramatically negative,  $w_a \lesssim -1$ , which is disfavoured in most quintessence-type models).

In Fig. 1 we also show contours of  $(1 + z_{\text{acc}})/E(z_{\text{acc}})$ , which is equivalent to the “net speedup” or integrated acceleration between  $z_{\text{acc}}$  and today; this is discussed later in § 3.

### 2.2 SN data

For comparison with models, we use the “Union 2.1” compilation of type-Ia SN distance moduli (Suzuki et al 2012), which contains 580 SNe of good quality spanning the range  $0.01 < z < 1.6$ . For plotting purposes we divide the sample into bins of approximately equal width in  $\ln(1 + z)$ , while adjusting bin widths so that each bin contains  $\geq 20$  SNe except at the highest redshifts; then, the mean distance modulus residual and weighted average redshift are computed for each bin. The resulting binned data points are shown as ‘Union 2.1’ in subsequent figures.

We show a fit of this data set to flat  $w$ CDM models (with  $\Omega_m$  and constant  $w$  as the fit parameters; results of this fit are shown in Fig. 2, with a best-fitting point near  $\Omega_m = 0.28$ ,  $w = -1.01$ . This shows the well-known degeneracy track between  $\Omega_m$  and  $w$ ; here we note that the long axis of the track is quite similar to the contour  $(1 + z_{\text{acc}})/E(z_{\text{acc}}) \approx 1.15$  in Fig. 1; this is discussed in later sections.

We note that a more recent SN Ia compilation has been produced by Betoule et al (2014) which includes more intermediate redshift SNe, more detailed photometric calibration and expanded treatment of systematic errors; however, the best-fitting parameters from the latter paper are within  $1\sigma$  of those above, so the slight difference is not important for the remainder of this paper.

### 2.3 Fiducial models and $\Delta\mu$

The observations of Type Ia SNe are sensitive to the standard luminosity distance  $D_L(z)$  for each SN, plus some scatter due to the intrinsic dispersion in absolute magnitude per

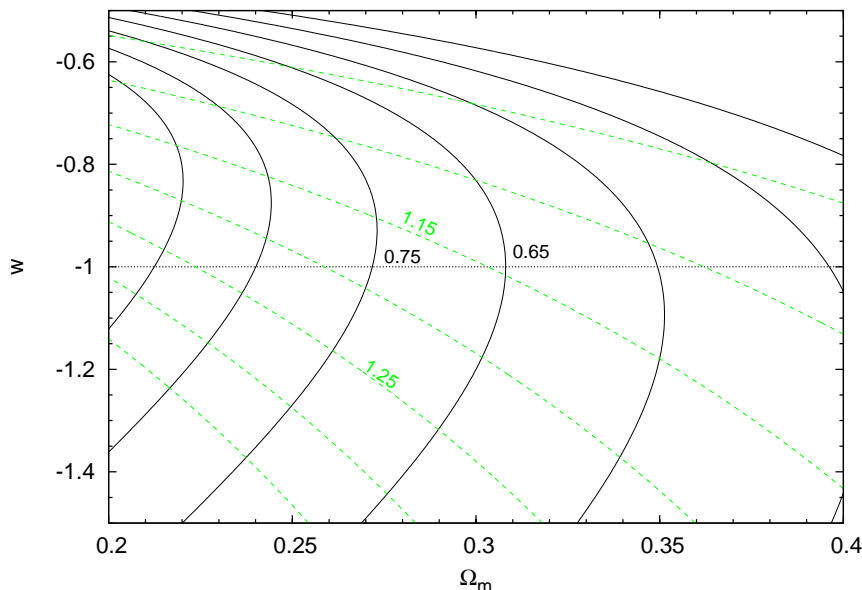


**Figure 1.** A contour plot of the acceleration redshift  $z_{\text{acc}}$ , and  $(1 + z_{\text{acc}})/E(z_{\text{acc}})$ , as functions of  $\Omega_m, w$  for flat  $w$ CDM models. The dotted horizontal line shows  $w = -1$ . The solid black contours show  $z_{\text{acc}}$ , in linear steps of 0.1 from 0.35 (right) to 0.95 (left). The dashed green contours show  $(1 + z_{\text{acc}})/E(z_{\text{acc}})$  (i.e. total net speed-up) in linear steps of 0.05 from 1.05 (upper right) to 1.35 (lower left). Selected contours are labelled.

SN. In practice, the distant  $z \gtrsim 0.1$  SNe are compared to a local sample “in the Hubble flow” typically at  $z \sim 0.02$  to  $0.05$ ; for the local sample, peculiar velocities are assumed to be relatively small compared to the cosmological redshift, so the value of  $H_0$  cancels with the (unknown) characteristic luminosity  $L_c$  of a standardized SN. Thus, quasi-local SNe really constrain the degenerate combination  $h^2 L_c$  or equivalently  $M_c + 5 \log_{10} h$ ; and comparison of distant and local SN samples actually constrains the distance ratio  $D_L(z)/D_L(z \sim 0.03)$ , rather than the absolute distance.

The value of  $D_L(z)$  spans a very wide range over the redshift interval covered by SNe: from  $z \sim 0.03$  to  $z \sim 2$  is a factor of  $\approx 118$  in distance or 10.3 magnitudes, while the differences between models are relatively modest: e.g. 15 percent differences between  $\Lambda$ CDM and a zero- $\Lambda$  open model, down to differences  $\sim 2$  percent between  $\Lambda$ CDM and a  $w = -0.9$  model. This implies that plotting  $D_L(z)$  versus  $z$  directly is not very informative since model differences are very small compared to the plot range; therefore it is common to present SN results as residuals relative to some fiducial model; residuals are often presented in distance modulus or magnitude units, i.e.

$$\Delta\mu(z) \equiv 5 \log_{10} \frac{D_L(z)}{D_{L,\text{fid}}(z)} \quad (3)$$

where  $D_{L,\text{fid}}$  is the value for some fiducial model. The choice of fiducial model is essentially arbitrary (up to small binning effects second-order in bin size); however, this choice can have a strong effect on the shape of the results and intuitive deductions, as shown below.

One obvious choice of fiducial is  $\Lambda$ CDM itself; however, this makes observed residuals (almost) flat-line, which does not translate readily into inferences on deceleration or acceleration. Another common choice of fiducial

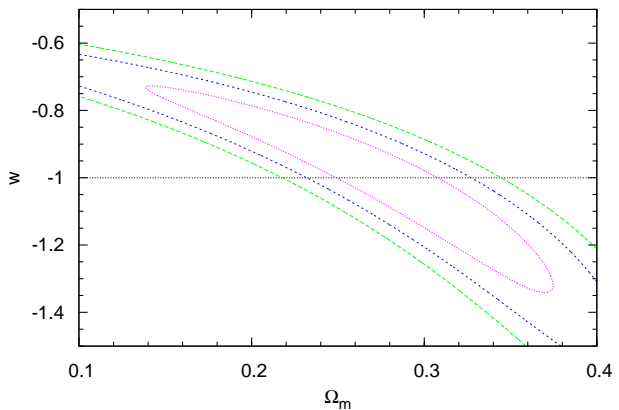


**Figure 2.** The allowed region in the  $(\Omega_m, w)$  plane from fitting flat constant- $w$  models to the Union 2.1 SN sample. Contours show the values of  $\Delta\chi^2 = 2.3, 6.0, 10.6$ , corresponding to 68, 95 and 99.8 percent confidence regions.

model is the empty or Milne model, with  $\Omega_m = 0$ ,  $\Omega_\Lambda = 0$ ,  $\Omega_k = 1$ , as used by many notable papers e.g. Riess et al (1998); Leibundgut (2001); Riess et al (2004); Goobar & Leibundgut (2011). The zero matter density means this is clearly not a viable model for the real Universe, but it is a convenient fiducial model for two reasons:

- (i) It has a very simple analytic form for  $D_L(z)$ , given by

$$D_{L,E}(z) = \frac{c}{H_0} z \left( 1 + \frac{z}{2} \right) ; \quad (4)$$

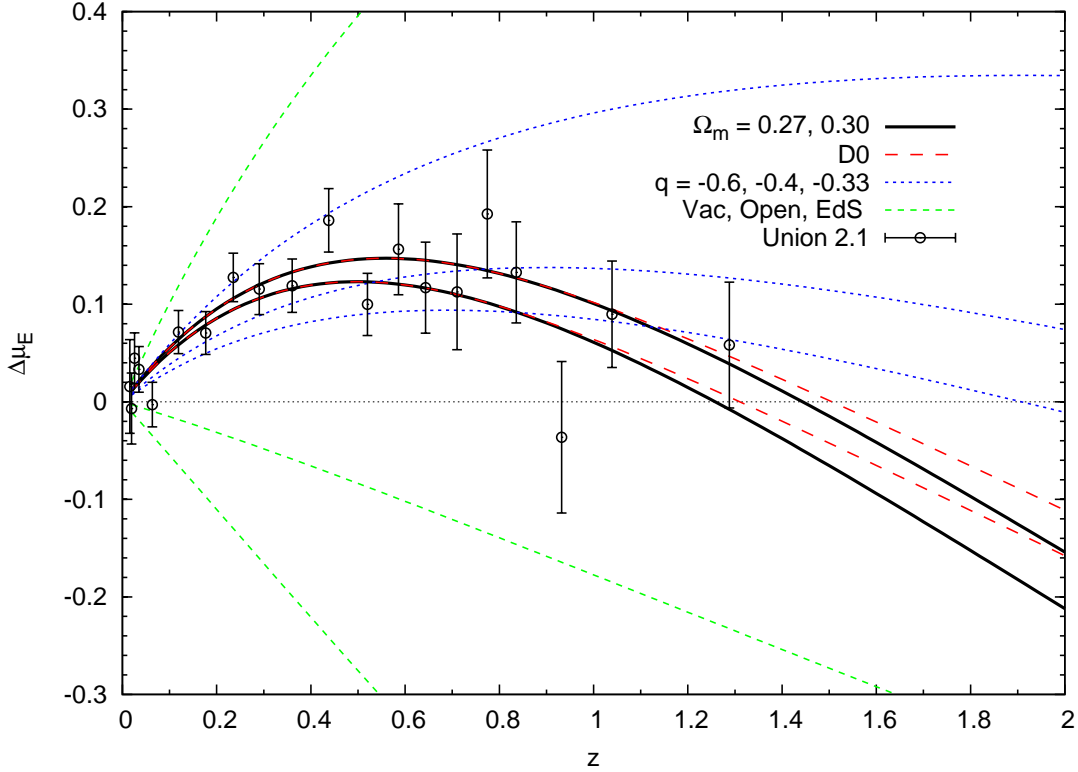


**Figure 3.** Distance modulus residuals relative to the Milne model for various cosmological models. The solid black lines show  $\Lambda$ CDM with  $\Omega_m = 0.27$  (upper) and  $0.30$  (lower). Long-dashed red lines show the corresponding D0 models (Equation 12) with deceleration artificially turned off above  $z_{\text{acc}}$ . Dashed green lines show Friedmann models of historical interest: from top to bottom, a pure-vacuum model ( $\Omega_\Lambda = 1$ ); an open model with  $\Omega_m = 0.27$ ,  $\Omega_\Lambda = 0$ ; and an Einstein-de Sitter model ( $\Omega_m = 1$ ). Dotted blue lines show constant- $q$  models with  $q_c = -0.6, -0.4, -0.33$  respectively (top to bottom).

hereafter we define  $\Delta\mu_E$  to be distance modulus residuals relative to this.

(ii) For a given  $H_0$ , the Milne model has the maximum luminosity distance among all Friedmann models with zero dark energy (assuming non-negative matter density). Therefore, observational evidence for distance ratios larger than the Milne model (positive  $\Delta\mu_E$ ) at any redshift is direct evidence that we do not live in a Friedmann model with zero dark energy.

However, using the Milne model as fiducial has some drawbacks which we discuss in the next subsection; we suggest an improved fiducial model in Section 3 (see also Mortsell & Clarkson 2009).

## 2.4 Downturn in distance residuals

It is very well known that observed SN distance residuals are all significantly positive at  $0.2 \lesssim z \lesssim 0.6$ , in agreement with the  $\Lambda$ CDM accelerating expansion. It is also fairly well known that  $\Lambda$ CDM models exhibit a turning point (a maximum) in the  $\Delta\mu_E(z)$  relation. Fig. 3 shows that this turning point, hereafter  $z_{tp}$ , occurs at  $z \simeq 0.50$  for the  $\Omega_m = 0.300$  concordance model, and the predicted residuals then decline to a zero-crossing at  $z \simeq 1.26$ . It is seen in Fig. 3 that the actual supernova data do hint at the existence of a turnover, with the three data points at  $z > 0.9$  all slightly low compared to their predecessors. The actual evidence for this turnover is not decisive, but it is clearly somewhat preferred by the data. The turnover occurs quite close to the theoretical transition epoch  $z_{\text{acc}} \approx 0.67$ , and it is therefore widely believed (at least anecdotally) that supernovae have directly detected the predicted cosmic deceleration at  $z \gtrsim 1$ . We discuss some prior claims to this effect in Appendix A.

We demonstrate in the next subsection that the latter conclusion does not follow; specifically, while a downturn in  $\Delta\mu_E$  is favoured by the data, the downturn predicted by  $\Lambda$ CDM is *mostly* caused by the negative space curvature in the fiducial Milne model, and cosmic deceleration makes only a minority contribution to the downturn. The fairly close match between  $z_{tp}$  and  $z_{\text{acc}}$  is found to be largely coincidental.

## 2.5 Cause of the turnover in $\Delta\mu_E$

Assuming homogeneity, the luminosity distance  $D_L(z)$  is given by

$$D_L(z) = \frac{c}{H_0}(1+z) \frac{1}{\sqrt{|\Omega_k|}} S_k \left( \sqrt{|\Omega_k|} \int_0^z \frac{dz'}{E(z')} \right) \quad (5)$$

with  $E(z) \equiv H(z)/H_0$ , and the function  $S_k(x) = \sin x, x, \sinh x$  for  $k = +1, 0, -1$  respectively, where  $k$  is the sign of the curvature (opposite to the sign of  $\Omega_k$ , in the usual convention where  $\Omega_k = 1 - \Omega_{\text{tot}}$ ).

It is convenient to factorize this so that

$$D_L(z) = (1+z) D_R(z) \left( \frac{S_k(x)}{x} \right) \quad (6)$$

$$D_R(z) = \frac{c}{H_0} \int_0^z \frac{dz'}{E(z')} = c \int_0^z \frac{dz'}{H(z')} \quad (7)$$

$$x \equiv \frac{H_0 D_R(z)}{c} \sqrt{|\Omega_k|} \quad (8)$$

where  $D_R(z)$  is the comoving radial distance to redshift  $z$ ; and  $x$  is the dimensionless ratio between  $D_R(z)$  and the cosmic curvature radius, which in a Friedmann model is  $R_c = c/H_0 \sqrt{|\Omega_k|}$ . We note that these distance results are still valid in a homogeneous and isotropic non-GR model, as long as the Robertson-Walker metric applies and we define  $\Omega_k$  from the curvature radius via  $\Omega_k \equiv \pm(H_0 R_c/c)^{-2}$ , which is then not necessarily equal to  $1 - \Omega_{\text{tot}}$ .

Looking at equation (6), the first  $(1+z)$  factor is parameter-independent and due to time-dilation and loss of photon energy; these each give one power of  $(1+z)^{-1}$  in flux, hence combine to  $(1+z)$  in equivalent distance. The parameter dependence of  $D_L(z)$  then factorizes into two parts, the  $D_R(z)$  term dependent only on expansion history, and the factor  $S_k(x)/x$  which depends mainly on curvature and also (more weakly) on expansion history; this is asymptotically  $1 - kx^2/6$  for  $x \ll 1$ , or  $1 + \Omega_k z^2/6$  for  $z \ll 1$ . The factorization above is helpful to understand the relative importance of curvature versus acceleration/deceleration on the distances and distance ratios. In the non-flat  $\Lambda$ CDM model, the combination of *Planck*+BAO data requires  $|\Omega_k| < 0.008$  at 95 percent confidence<sup>2</sup>, (see equations 68a and b of Planck Collaboration (2014)), which implies that the curvature factor is within 0.2 percent of 1 at the redshift range  $z \lesssim 1.5$  of current SNe.

It is now interesting to compare terms in equation (6) for the  $\Lambda$ CDM and empty models. In the case of the empty model,  $D_R(z) = (c/H_0) \ln(1+z)$ ,  $\Omega_k = +1$ , so equation (6) becomes

$$D_{L,E}(z) = (1+z) \frac{c}{H_0} \ln(1+z) \frac{\sinh(\ln(1+z))}{\ln(1+z)} \quad (9)$$

<sup>2</sup> We note that in non-GR models the standard limits on  $\Omega_k$  does not apply; however, if the true cosmology were a curved non-GR model, if  $|\Omega_k| \gtrsim 0.05$  we would then require a rather close cancellation between curvature and non-GR effects in order to make the non-flat  $\Lambda$ CDM fits turn out so close to  $\Omega_k = 0$ . If we discard this possibility as an unnatural conspiracy, it is reasonable to assume  $|\Omega_k| < 0.05$ , and in that case the curvature factor  $S_k(x)/x \approx 1 \pm 0.01$  for  $z < 1.5$  for reasonable expansion histories.

which easily simplifies to equation (4). However, it is more informative to keep the longer form of equation (9) since the rightmost fraction is a pure curvature effect; it is well approximated by  $1 + (\ln(1+z))^2/6$  at  $z \lesssim 1$ . We next show that this term, *not* the transition to deceleration, is the dominant cause of the downturn in  $\Delta\mu_E$  for models similar to  $\Lambda$ CDM.

Considering the distance modulus residual  $\Delta\mu$  for any flat model relative to the empty model, we then have

$$\Delta\mu_E(z) = 5 \log_{10} \left[ \frac{\int_0^z \frac{1}{E(z')} dz'}{\ln(1+z)} \frac{\ln(1+z)}{\sinh(\ln(1+z))} \right] \quad (10)$$

$$\equiv \Delta\mu_H(z) - \Delta\mu_k(z) \quad (11)$$

where we have broken the  $\Delta\mu_E$  into two additive terms,  $\Delta\mu_H(z) \equiv 5 \log_{10} [\int_0^z (1/E(z')) dz' / \ln(1+z)]$  due to expansion histories, and  $\Delta\mu_k(z) \equiv 5 \log_{10} [\sinh(\ln(1+z)) / \ln(1+z)]$  is the term due to curvature in the empty model (here defined so  $\Delta\mu_k$  is positive, thus it is subtracted in equation (11) above).

For illustration, we evaluate each of these terms for  $\Lambda$ CDM (with  $\Omega_m = 0.30$ ) at two specific redshifts: we choose  $z_a = 0.50$  close to the turning point, and  $z_b = 1.26$  to be the downward zero-crossing where  $\Delta\mu_E(z) = 0$ . We then find  $\Delta\mu_E(0.50) = 0.1231 = 0.1822 - 0.0592$  where the latter two are  $\Delta\mu_H$  and  $\Delta\mu_k$  respectively. At  $z_b = 1.26$  we find  $-0.0005 = 0.2350 - 0.2355$ . Note that  $\Delta\mu_H$  grows from  $z = 0.50$  to  $z = 1.26$ , since although the expansion is decelerating over most of this interval, the expansion rate  $\dot{a}$  remains smaller than the present-day value; see below.

For comparison purposes, it is useful to evaluate how much the predicted deceleration contributes to  $\Delta\mu_H$ : for this we define another model set, hereafter D0, which exactly matches  $\Lambda$ CDM back to  $z_{\text{acc}}$  but with deceleration artificially switched off ( $q = 0$ ) at  $z > z_{\text{acc}}$ : specifically, we define model D0 by

$$\begin{aligned} H(z) &= H_{\Lambda\text{CDM}}(z) \text{ if } z \leq z_{\text{acc}} \\ &= H_{\Lambda\text{CDM}}(z_{\text{acc}})(1+z)/(1+z_{\text{acc}}) \text{ if } z > z_{\text{acc}} \end{aligned} \quad (12)$$

The D0 models are somewhat artificial, but have a continuous  $q(z)$  and are useful to isolate the relative contribution of  $\Lambda$ CDM deceleration on the observables. Also, they represent in a sense the closest possible match to  $\Lambda$ CDM among all possible non-decelerating models, so they are an interesting target to attempt to exclude observationally. The D0 model (for  $\Omega_m = 0.30$ ) is identical to the corresponding  $\Lambda$ CDM at  $z_a$ , and at  $z_b$  we find  $\Delta\mu_H = 0.2464$  (and  $\Delta\mu_k = 0.2355$  again). Therefore, the actual brightening effect attributable to deceleration in  $\Lambda$ CDM is just the difference in  $\Delta\mu_H$  between  $\Lambda$ CDM and D0, which is only  $-0.011$  mag. This is smaller by a factor of 20 than the curvature effect; so, the bottom line of this subsection is that at  $z = 1.26$ , 95% of this downturn is due to curvature in the empty fiducial model (or 90% if we divide by the value  $\Delta\mu_E = 0.1231$  mag at its maximum). Either way, it is clear that the open curvature in the Milne model greatly dominates over deceleration as the source of the downturn in  $\Delta\mu_E$ .

### 3 AN IMPROVED FIDUCIAL MODEL

#### 3.1 The flat non-accelerating model

We have argued above that the presentation of distance residuals from the Milne or empty model is potentially confusing, since it leads to a generic curvature-induced downturn in the residuals at  $z \gtrsim 0.5$  which occurs *independent* of whether the expansion really decelerated prior to that epoch. In this section we look at an improved fiducial model and demonstrate several advantages.

In particular, the above discussion suggests a natural fiducial model is one with a constant expansion rate (deceleration parameter  $q(z) = 0$ , and  $H(z) = H_0(1+z)$  at all redshifts, as for the Milne model), but simply setting curvature to zero (equivalent to striking out the  $\sinh$  in the equations above). This is equivalent to a Friedmann model with  $\Omega_m = 0$ ,  $\Omega_{DE} = 1$  and  $w = -1/3$ ; hereafter model N for short. (This reference model has been employed previously by Seikel & Schwarz (2008) and Mortsell & Clarkson (2009), but appears to be rather uncommon in the literature.) Again, this model is not realistic due to the zero matter density, but it is useful since it has both zero deceleration and zero curvature. This model straightforwardly gives

$$D_{L,N}(z) = \frac{c}{H_0}(1+z) \ln(1+z). \quad (13)$$

We now define the distance ratio for any other model,  $y_D(z)$ , as the ratio  $D_L(z)/D_{L,N}(z)$ , therefore

$$y_D(z) \equiv \frac{H_0 D_R(z)}{c \ln(1+z)} \frac{S_k(x)}{x} \quad (14)$$

For an almost-flat model at  $z \lesssim 1.7$  we can again neglect the curvature term as very close to 1 (as per footnote in Sect. 2.5)

Thus, for flat models the distance ratio becomes

$$y_D(z) = \frac{1}{\ln(1+z)} \int_0^z \frac{dz'}{E(z')} \quad (15)$$

For many purposes below, it is more convenient to change the redshift variable to  $u = \ln(1+z)$ , which gives

$$y_D(u) = \frac{1}{u} \int_0^u \frac{1+z'}{E(z')} du'; \quad (16)$$

as usual  $u', z'$  are dummy integration variables, not derivatives, and  $y_D(u)$  means  $y_D(z = e^u - 1)$ .

This  $y_D$  is directly related to  $\Delta\mu_H$  above via  $\Delta\mu_H(z) = 5 \log_{10} y_D(z)$ , but several results below are simplified if we choose *not* to apply this log. Since  $y_D(z)$  is fairly close to 1 in reasonable models, this is anyway rather close to a linear stretch  $\Delta\mu_H \approx 2.17(y_D - 1)$ .

Since  $E(z)/(1+z)$  is just the expansion rate at  $z$  relative to the present day, i.e.  $\dot{a}(z)/\dot{a}(z=0)$ , the integrand of equation (16) is just the inverse of this; i.e.  $y_D(z)$  measures the average value of  $(\dot{a})_0/\dot{a}$  with respect to  $\ln(1+z)$ , over the interval from the source to the present. It is more convenient to work with averages of  $(1+z)/E(z)$  rather than  $1/E(z)$ , since the former varies much more slowly with redshift: for our default  $\Lambda$ CDM model,  $(1+z)/E(z)$  reaches a maximum value of 1.153 at  $z_{\text{acc}} \simeq 0.67$ , crosses 1 again at  $z \simeq 2.08$ , and declines to 0.895 at  $z = 3$ .

Note also that since  $(1+z)/E(z)$  contains the inverse

of  $\dot{a}$ , while  $z$  increases backwards in time, derivatives of  $(1+z)/E(z)$  have the same sign as  $\ddot{a}$ , i.e. positive for acceleration. In fact the standard deceleration parameter  $q \equiv -\ddot{a}/(aH^2(a))$  is given by

$$q(u) = -\frac{d}{du} \ln \left( \frac{1+z}{E(z)} \right) \quad (17)$$

which is useful below.

#### 3.2 Useful properties of $y_D$

The above definition of  $y_D$  is simple and intuitive, and we show below that it enables a number of useful non-parametric deductions, as follows:

(i) It is clear above that a value of  $y_D(z) > 1$  at any  $z$  implies the past-average of  $\dot{a}$  was less than the present value, i.e. acceleration has dominated over deceleration over this interval (note, this is not strictly the same as requiring  $\ddot{a} > 0$  at the present day); this feature is similar to the Milne fiducial model above.

(ii) It is easy to see that if  $q(z)$  is always negative over some interval  $0 \leq z \leq z_1$ , then  $(1+z)/E(z)$  is a strictly increasing function of  $z$ , and therefore so is  $y_D(z)$ ; i.e. a flat model which is non-decelerating at  $0 < z < z_1$  cannot have a turnover in  $y_D$  at  $z \leq z_1$ , regardless of the specific expansion history. The converse of this is that *if* a turnover in  $y_D(z)$  is observed, this implies a transition to deceleration must have occurred within the interval, i.e. we can definitely conclude  $z_{\text{acc}} < z_{tu}$  independent of the functional form of  $E(z)$ . Also, if a turnover exists at  $z_{tu}$ , differentiating equation (16) implies that the value of  $1/\dot{a}$  at  $z_{tu}$  was equal to its average value (w.r.t.  $u$ ) across the interval from  $z_{tu}$  to today.

(iii) We can improve on the results above using the Mean Value Theorem: specifically, if had a known value  $y_D(z_1) = y_1$ , this theorem implies that there exists some  $z < z_1$  with  $(1+z)/E(z) \geq y_1$ ; i.e. the cosmic expansion rate has speeded up by at least a factor of  $y_1$  since some  $z < z_1$ , independent of the functional form of  $E(z)$ . For a more realistic case where we measure an average value of  $y_D$  in a finite bin, e.g.  $\langle y_D \rangle = \hat{y}$  averaged between  $z_1 < z < z_2$ , we can use the Mean Value Theorem *twice*: first, there exists some  $z_m$  within this bin with  $y_D(z_m) = \hat{y}$ , and secondly there exists some  $z_3 \leq z_m \leq z_2$  satisfying  $(1+z_3)/E(z_3) \geq \hat{y}$ . The above argument applies for exact knowledge of  $\hat{y}$ , neglecting error bars; however, it is clear that the same argument also applies if we insert an observational lower bound for  $\hat{y}$ .

(iv) Also, it is interesting to ask a reverse question: if the expansion was decelerating at all  $z > z_{\text{acc}}$ , does this imply that a turnover in  $y_D(z)$  must exist? The answer appears to be ‘almost always’: it is possible to build a contrived expansion history where  $q(z)$  crosses from negative to a small positive value, then asymptotes back to zero from above at high  $z$ , so  $(1+z)/E(z)$  tends to a constant from above; in this contrived case we can have deceleration at all  $z > z_{\text{acc}}$  while  $y_D(z)$  monotonically increases to the same constant. However, if we assume non-infinitesimal deceleration,  $q(z) \geq +\epsilon$  for all  $z > z_1$  and some positive value  $\epsilon$ , it is readily proved that  $y_D(z)$  must have a turnover at some  $z$  (though not necessarily in a readily observable range).

(v) Differentiating equation (16) and rearranging gives

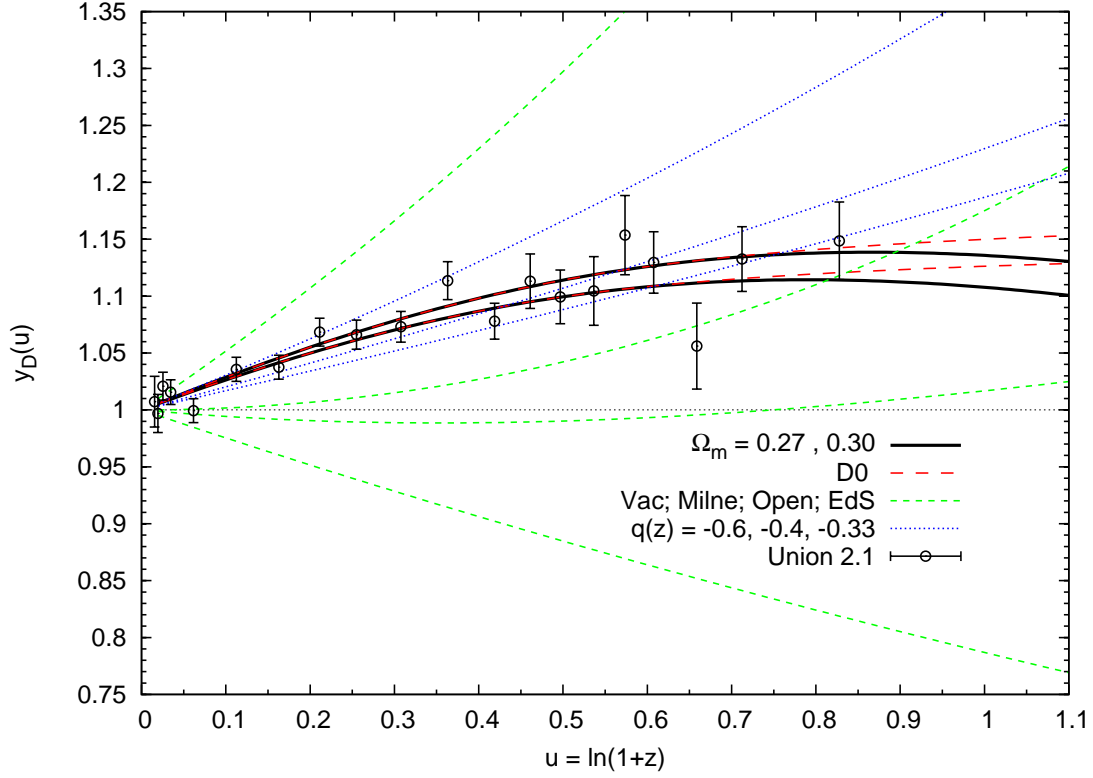


**Figure 4.** As Fig. 5, but with the horizontal axis now linear in  $u = \ln(1+z)$ .

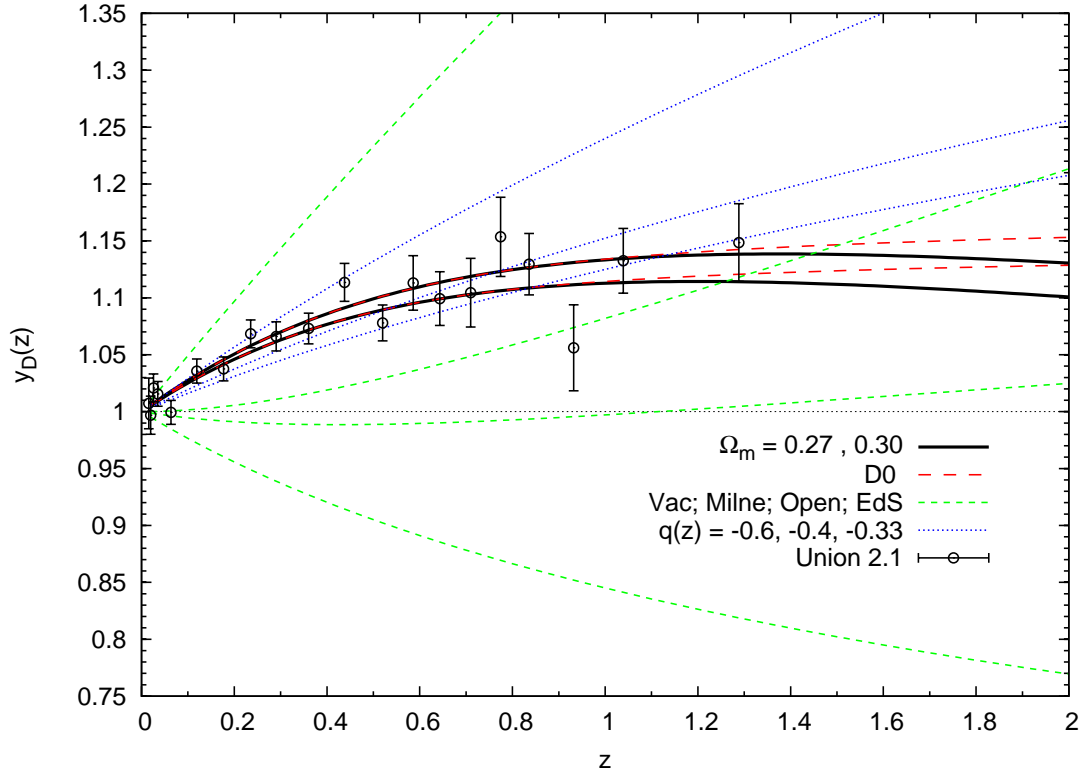


**Figure 5.** The distance ratio  $y_D(z)$  defined in equation (14) for various cosmological models. As in Fig. 3, solid black lines are  $\Lambda$ CDM models with  $\Omega_m = 0.27$  (upper) and  $0.30$  (lower). Long-dashed red lines are corresponding D0 models, with deceleration artificially switched off. The short-dashed green lines are four Friedmann models of historical interest: from top to bottom, vacuum-dominated ( $\Omega_m = 0, \Omega_\Lambda = 1$ ); empty (Milne); open ( $\Omega_m = 0.27, \Omega_{DE} = 0$ ); and Einstein-de Sitter ( $\Omega_m = 1$ ). Dotted blue lines are three constant- $q$  models with  $q = -0.6, -0.4, -0.33$  (top to bottom). Points with errorbars show the binned Union 2.1 SNe data.

$$\frac{1+z}{E(z)} = y_D(u) + u \frac{dy_D}{du}. \quad (18)$$

This gives us a direct graphical implication: taking the tangent to the curve of  $y_D(u)$  at any point  $u_1$  and extrapolating the tangent line to  $u = 2u_1$  gives us directly the value of  $(1+z)/E(z)$  at  $z_1 = \exp(u_1) - 1$ .

Differentiating again shows that the transition to acceleration occurs when  $d^2 y_D/du^2 = -(2/u)dy_D/du$ ; however, as is well known the need to take a second derivative of noisy data implies that this is not a very useful method for directly estimating  $u_{acc}$ .

(vi) Substituting from equation (17) above leads to the compact results

$$y_D(u) = \frac{1}{u} \int_0^u \exp \left[ - \int_0^{u'} q(u'') du'' \right] du', \quad (19)$$

$$q(u) = \frac{-2 \frac{dy_D}{du} - u \frac{d^2 y_D}{du^2}}{y_D(u) + u \frac{dy_D}{du}}; \quad (20)$$

this shows that  $q_0 = -2(dy_D/du)(0)$ , but also that as  $u$  increases we get increasing weight from the second-derivative term, so it becomes increasingly more challenging to constrain  $q(u)$  directly from numerical derivatives of data with realistic noise. Even for optimistic 1% error bars on  $y_D$  in bins  $\Delta u = 0.1$ , we get order-unity errors on  $d^2 y_D/du^2$ , so free-form reconstruction of  $q(u)$  is essentially impossible given realistic errors; the best we can do is assume some smooth few-parameter model for  $q(u)$  and fit.

(vii) From equation (16) it clearly follows that for two measurements at redshifts corresponding to  $u_1, u_2$  we have

$$\frac{u_2 y_D(u_2) - u_1 y_D(u_1)}{u_2 - u_1} = \frac{1}{u_2 - u_1} \int_{u_1}^{u_2} \frac{1+z'}{E(z')} du' \quad (21)$$

where the right-hand side (RHS) is the average of  $(1+z)/E(z)$  between the endpoints; therefore we can estimate this average as a linear combination of the two values at the ends; this is simple with respect to combination of error bars, and does not assume  $u_2 - u_1$  is small.

(viii) We now show another useful property of  $y_D$ : for any flat model with  $q(z) = \text{constant}$  (of either sign), the second derivative  $d^2 y_D/du^2$  with respect to  $u$  is everywhere non-negative. For such a model, denoting  $q_c$  as the constant value of  $q$ , we have  $H(z) = H_0(1+z)^{1+q_c}$ . This easily leads to

$$D_L(z) = \frac{c}{H_0} (1+z)^{-\frac{1}{q_c}} [(1+z)^{-q_c} - 1] \quad (22)$$

$$y_D(z) = \frac{-1}{q_c} \frac{(1+z)^{-q_c} - 1}{\ln(1+z)} \quad (23)$$

$$y_D(u) = \frac{1 - e^{-q_c u}}{q_c u} \quad (24)$$

Now differentiating twice with respect to  $u$  gives

$$\frac{d^2 y_D}{du^2} = \frac{-1}{q_c} \left[ \frac{e^{-q_c u} (u^2 q_c^2 + 2u q_c + 2) - 2}{u^3} \right] \quad (25)$$

$$= q_c^2 \left[ \frac{2 - e^{-p} (p^2 + 2p + 2)}{p^3} \right] \quad (26)$$

where we define  $p \equiv q_c u$ . The function in square brackets above is positive for all  $p$ , thus the above second derivative is everywhere non-negative for any value of  $q_c$  with either

sign, and is zero only if  $q_c = 0$  and  $y_D \equiv 1$ . For the cases of interest here, we are mainly interested in  $-0.6 < q_c < 0$  at  $0 < u < 1$ , hence  $-0.6 < p < 0$ ; the square-bracket term evaluates to  $1/3$  for  $p = 0$  and  $0.53$  for  $p = -0.6$ , so for any reasonable  $q_c$  model the second derivative is then between  $0.33q_c^2$  and  $0.53q_c^2$ , i.e. small, positive and slowly varying with  $u$ .

This has a useful consequence: if  $q(u)$  were in fact any constant, then the graph of  $y_D(u)$  versus  $u$  must always show positive curvature (concave from above). Conversely, if the observed data points for  $y_D(u)$  exhibit significant negative curvature over some interval, we can conclude that  $q(u)$  increased with  $u$  at some point within the observed interval, again regardless of the specific functional form. (Note this does not necessarily imply that  $q(u)$  became positive, merely that it increased with  $u$  i.e. was less negative in the past.)

We note that in the above points, items (i)-(iv) apply whether we choose  $z$  or  $u$  as the redshift variable, but items (v)-(viii) only apply with  $u$  as the variable; this suggests the latter is preferred.

For an illustration of the current data, we plot  $y_D(u)$  against  $u = \ln(1+z)$  in Fig. 4. Although this is a simple transformation of the  $x$ -axis from Fig. 5, the qualitative appearance is somewhat different due to the non-linear transformation, i.e. higher redshifts become squashed. The apparent ‘‘knee’’ in the  $\Lambda$ CDM models around  $z \sim 0.5$  in Fig. 5 is significantly smoothed out with the  $u$ -axis, and both  $\Lambda$ CDM models now look very close to simple parabolas (see below). Also, the constant- $q$  models change curvature from negative in Fig. 5 to small and positive in Fig. 4, as derived above. Comparing to the data, it is clear that the SNe data points do marginally prefer a negative curvature in  $y_D(u)$ , but not overwhelmingly so.

To quantify this, we fit three models to the  $y_D(u)$  data points: a linear model, a quadratic, and the family of constant- $q$  models above; we find that the quadratic model is preferred over the linear model by  $\Delta\chi^2 = 3.5$  for 1 extra degree of freedom (d.o.f.), while the quadratic is preferred over the best constant- $q$  model by  $\Delta\chi^2 = 5.7$  for 1 extra d.o.f. This indicates that negative curvature in  $y_D$  (increasing  $q$ ) is preferred, but only at around the  $2\sigma$  significance level. We expand on the quadratic model below.

### 3.3 A quadratic fitting function for $(1+z)/E(z)$

Here we note that it is interesting to consider a fitting function where  $1/\dot{a}$  is a quadratic function of  $u$ , specifically

$$\frac{1+z}{E(z)} = 1 + b_1 u - b_2 u^2 \quad (27)$$

with arbitrary constants  $b_1, b_2$ , and  $u \equiv \ln(1+z)$  as before. The minus sign above is chosen so that positive  $b_1, b_2$  leads to recent acceleration and past deceleration as anticipated, with  $u_{acc} = b_1/2b_2$  from equation (17). This fitting function is not physically motivated, but is useful since it provides a very good approximation to models similar to  $\Lambda$ CDM at  $u < 1$ , ( $z < 1.72$ ) (see Appendix C for an approximate explanation of this property), and it gives several simple analytic results below.

Fitting this function to the default  $\Lambda$ CDM  $(1+z)/E(z)$  over  $0 < u < 1$  ( $z < 1.72$ ) gives best-fitting values  $b_1 =$



0.569,  $b_2 = 0.530$  with an rms error of 0.28 percent, and a worst-case error of  $-0.8$  percent. (This fit becomes significantly worse above  $z \gtrsim 2$ , and has a catastrophic zero-crossing at  $u \sim 2$  ( $z \sim 6.4$ ), but it is good over the range accessible to medium-term SN data.) The functional form (27) gives simple relations between  $u_{\text{acc}}$  and the turnover in  $y_D$ ; it easily gives

$$y_D(u) = 1 + \frac{1}{2}b_1u - \frac{1}{3}b_2u^2; \quad (28)$$

$$q(u) = \frac{-b_1 + 2b_2u}{1 + b_1u - b_2u^2}; \quad (29)$$

$$D_L(u) = \frac{c}{H_0}(1+z)(u + \frac{1}{2}b_1u^2 - \frac{1}{3}b_2u^3); \quad (30)$$

so  $y_D(u)$  is also an exact quadratic in this case. The  $q(u)$  behaviour is approximately linear at moderate  $u$ , so this model is fairly similar to the model  $q(a) = q_0 + q_a(1-a)$  used elsewhere. Equation (30) with values  $b_1, b_2$  as above matches the exact numerical  $D_L(z)$  for  $\Lambda$ CDM with very high accuracy, a maximum error only 0.13 percent back to  $u = 1$ ; this error is substantially smaller than for  $E(z)$ , due to the integral for  $D_L$ .

We find that the results above also work well for  $w$ CDM models in the region  $0.2 < \Omega_m < 0.4$ ,  $-1.2 < w < -0.8$ ; thus, it is interesting (and partly a coincidence) that any  $w$ CDM model within the presently-favoured range leads to a  $y_D(u)$  curve virtually indistinguishable from a quadratic, to around the 0.2 percent level i.e. comparable to the line thickness in Fig. 4. This gives another helpful feature: any proof of ‘percent-level’ deviation of  $y_D(u)$  from a simple quadratic would signify a failure of  $w$ CDM.

We now look at the relation between  $z_{\text{acc}}$  and the turning point in  $y_D$ . In the above model equation (27) with  $b_1, b_2 > 0$ , recall the acceleration epoch is  $u_{\text{acc}} = b_1/2b_2$ , hence  $(1+z_{\text{acc}})/E(z_{\text{acc}}) = 1 + b_1^2/4b_2$ ; while the maximum in  $y_D$  occurs at  $u_{\text{tp}} = 3b_1/4b_2$ , at height  $y_D(u_{\text{tp}}) = 1 + 3b_1^2/16b_2$ . So, in this model  $z_{\text{acc}}$  is directly related to the location  $u_{\text{tp}}$  of the maximum, and  $(1+z_{\text{acc}})/E(z_{\text{acc}})$  is directly related to its height, via

$$u_{\text{acc}} = \frac{2}{3}u_{\text{tp}}, \quad z_{\text{acc}} = (1 + z_{\text{tp}})^{2/3} - 1; \quad (31)$$

$$\frac{1 + z_{\text{acc}}}{E(z_{\text{acc}})} = 1 + \frac{4}{3}(y_D(u_{\text{tp}}) - 1) \quad (32)$$

without requiring to solve for  $b_1, b_2$ .

This suggests that for other reasonably smooth parametrizations of  $E(z)$  such as  $w$ CDM models, we may expect equations (31) and (32) to hold approximately, rather than exactly as above. In our default  $\Lambda$ CDM model, the exact values are  $z_{\text{acc}} = 0.671$ ,  $(1 + z_{\text{acc}})/E(z_{\text{acc}}) = 1.1530$ , while from numerical evaluation of  $u_{\text{tp}}$  and  $y_D(u_{\text{tp}})$  the RHS of the above equations evaluate to 0.693 and 1.1525 respectively; thus equation (31) is quite good, while equation (32) is an excellent approximation. More generally, we have tested these for  $w$ CDM models (constant  $w$ ) with the results shown in Fig. 6; this shows that equation (32) remains very accurate for a substantial range around the concordance model.

We have also tested linear- $q$  models  $q(a) = q_0 + q_a(1-a)$ , and find that equation (32) is accurate to better than 0.01 for reasonable values of  $q_0, q_a$ , while equation (31) is somewhat worse but generally good to a few percent. For varying- $w$

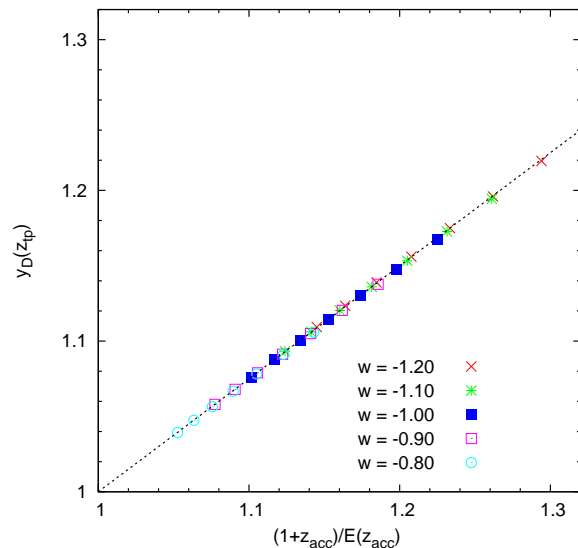


**Figure 6.** This figure shows the peak value of  $y_D$  against the integrated acceleration  $(1 + z_{\text{acc}})/E(z_{\text{acc}})$ , for a grid of  $w$ CDM models. The differing point styles show  $w = -1.2, -1.1, -1.0, -0.9, -0.8$  as indicated in the key. For each value of  $w$  we show seven points with  $\Omega_m = 0.24, 0.26, \dots, 0.36$  in linear steps of 0.02; in each case these run from  $\Omega_m = 0.24$  at upper-right to 0.36 at lower-left, so the central point is  $\Omega_m = 0.30$ . The dotted line (not a fit) is equation (32).

models of the form  $w(a) = w_0 + w_a(1-a)$ , these approximations remain good for  $w_a \geq 0$  but become somewhat less accurate for negative  $w_a$ , especially for  $w_a < -0.5$ .

The summary here is that equation (32) is generally an excellent approximation for constant- $w$  models, and a good approximation for varying- $w$  if  $w_a$  is not too negative; while equation (31) is fairly good at the few-percent level.

These approximations are useful since the right-hand-side of equations (31) and (32) are in principle directly observable: it is clear from Fig. 4 that the location of the possible maximum in  $y_D$  is relatively poorly constrained, but *if* the suggestion of negative curvature in  $y_D$  is real and persists as expected to higher redshifts, then the SNe datapoints imply that  $y_D(u)$  is probably approaching a maximum value  $\sim 1.10 - 1.14$  at  $u_{\text{tp}} \lesssim 1$ ; if so, this would give a direct and reasonably model-independent inference of the integrated acceleration  $(1 + z_{\text{acc}})/E(z_{\text{acc}}) \approx 1.13 - 1.18$ . This provides a useful intuitive explanation of the ridge-line of  $\Omega_m$  versus  $w$  observed in Fig. 2.

To summarize this subsection, we find that  $w$ CDM models with constant  $w$  near the concordance model are very well approximated by the above fitting functions, i.e. very close to simple quadratics in  $y_D(u)$ , and thus equations (31) and (32) provide quite accurate approximations relating the observable turning point in  $y_D$  to  $z_{\text{acc}}$  and the net acceleration.

Finally, in Appendix B we use the fitting function of equation (27) to provide a simple and accurate ‘computer-free’ approximation to the luminosity distance in  $w$ CDM models.

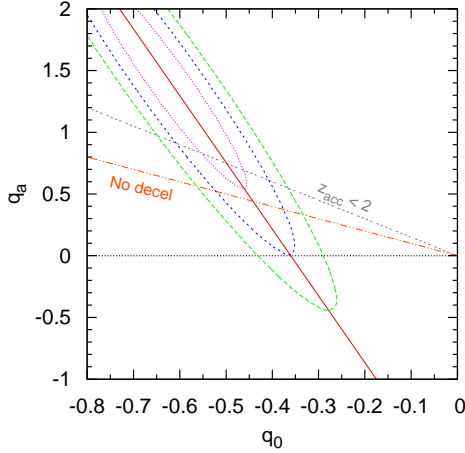


**Figure 7.** The allowed region in the  $(q_0, q_a)$  plane from fitting models with  $q(a) = q_0 + q_a(1 - a)$  to the Union 2.1 supernova data. Elliptical contours show the values of  $\Delta\chi^2 = 2.3, 6.0, 10.6$  corresponding to 68, 95 and 99.8 percent confidence regions. The sloping lines bound the region of no deceleration and the region  $z_{\text{acc}} < 2$ , with the wedge between these giving  $z_{\text{acc}} > 2$ . The line along the major axis of the ellipse is illustrative and gives a pivot value  $q(a = 0.815) = -0.36$  at  $a = 0.815$  ( $z = 0.227$ ).

### 3.4 Linear $q(a)$ models

Here we briefly consider the two-parameter model family with deceleration parameter  $q$  given by a linear function of scale factor  $a$ , i.e.

$$q(a) = q_0 + q_a(1 - a) \quad (33)$$

for constants  $q_0, q_a$ . This model has been used before by various authors (e.g. Cunha & Lima 2008, Santos et al 2011), since it is simple, fairly flexible and can produce a fairly good approximation to the behaviour of many dark energy models at  $z \lesssim 2$ . We have fitted this parameter pair to the Union 2.1 SN data, with best-fit values at  $(-0.62, +1.40)$  and the resulting likelihood contours shown in Fig. 7; as expected, negative  $q_0$  is required at very high significance. (This agrees well with a similar figure in Santos et al (2011)). The figure also shows lines bounding the regions of no past deceleration  $q_0 + q_a < 0$ , and the region  $z_{\text{acc}} < 2$  equivalent to  $q_0 + 2q_a/3 > 0$ ; the wedge between these lines corresponds to a transition redshift  $z_{\text{acc}} > 2$ . This plot shows that the no-deceleration region is disfavoured at around the  $1.3\sigma$  confidence level, but there is a region inside the wedge  $z_{\text{acc}} > 2$  which is allowed at around  $0.8\sigma$ . In this wedge, no deceleration occurs within the redshift range of observed SNe, so the inference of deceleration relies on a linear extrapolation of the  $q(a)$  model beyond the range of SNe. This generally agrees with our previous conclusions, that a trend of less negative  $q$  at higher redshift is clearly preferred, but there is negligible evidence from SN data alone for an actual transition to deceleration within the observed range.

## 4 DISCUSSION

It is instructive to blink back and forth between Figs 3, 5, 4 above: although from a parameter-fitting perspective there is no difference since the residuals (data–model) are all the same, from the perspective of visual intuition about expansion rate there are rather striking differences between these three Figures. Clearly, Fig. 3 shows a fairly convincing turnover in the data points; while in Fig. 5 the data shows negligible evidence for a turnover, but a reasonably convincing change in slope to a broad near-flat “plateau” above  $z \gtrsim 0.6$ . Finally, in Fig. 4 the  $\Lambda$ CDM models are extremely close to parabolic (i.e. near-constant negative second derivative), while the data points show near-linear behaviour with a reasonable but non-decisive indication of negative curvature; the constant- $q$  models show weak positive curvature as derived earlier in equation (18). As we argued earlier, the turnover in Fig. 3 is largely attributable to the negative space curvature in the Milne model, not due to actual deceleration. Figs 5 and 4 show a much more gradual turnover in the  $\Lambda$ CDM models, while the D0 models show the expected gradual rise; clearly the current data are completely unable to discriminate between  $\Lambda$ CDM and D0 models. We suggest that Fig. 4 is the most informative due to the various useful intuitive properties outlined in § 3.2 above.

The above conclusions seem somewhat unexpected: there is a widespread view (see Appendix A) that the SN data has convincingly verified the expected deceleration of the universe at  $z \gtrsim 1$ . However from the discussion above, the SNe data are almost entirely inconclusive on the sign of  $q$  at  $z > 0.7$ , and even a constant- $q$  model with  $q(z) \approx -0.4$  back to  $z \gtrsim 1$  is only excluded at the  $\sim 2.5\sigma$  level which is significant but not overwhelming. Thus, there is moderately good evidence for  $q$  increasing in the past, but concluding that  $q$  actually crossed zero to a positive value relies strongly on a smooth extrapolation of this trend, and is therefore model-dependent.

Conversely, if we assume GR, almost all the acceptable models imply significant deceleration at  $z > 1$ . Essentially, if we assume GR with the weak energy condition and a value of  $\Omega_m > 0.2$ , then the eightfold increase in  $\rho_m$  back to  $z = 1$  combined with the much slower increase in dark energy guarantees matter domination and deceleration at  $z > 1$ ; in this case deceleration at  $z > 1$  is mainly a prediction of GR, rather than a feature directly required by data. For the value of  $z_{\text{acc}}$  it is important to keep clear the distinction between an extrapolation based on GR parameter-fitting, or an actual detection purely based on data.

It is clear that the CMB does provide much stronger constraints due to the long distance lever-arm: if we assume the standard sound horizon length inferred from *Planck*, then we deduce  $y_D(z \simeq 1090) \simeq 0.44$ , which clearly requires a turnover and hence deceleration. However, since the CMB only gives us one integrated distance to  $z \sim 1090$  spanning seven  $e$ -folds of expansion, while the supernova data constrains only the last one  $e$ -fold of expansion, it would be straightforward to construct ‘designer’ expansion histories with some extra deceleration hidden in the un-observed six  $e$ -folds to offset an absence of deceleration back to  $z \sim 1.7$ . This is clearly contrived, but would not directly conflict with any available  $D_L(z)$  data. Therefore, even adopting the standard distance constraint from the CMB, we do not yet have

a GR-independent proof that the expansion was actually decelerating at  $1 \lesssim z \lesssim 2$ ; this is clearly the most probable and least contrived interpretation, but loopholes remain.

We note that recent BAO results do provide significant evidence for deceleration; from the first detection of BAOs in the Ly- $\alpha$  forest by Busca et al (2013) and comparison with lower-redshift measurements, Busca et al (2013) quote

$$\frac{E(z=2.3)/3.3}{E(z=0.5)/1.5} = 1.17 \pm 0.05 \quad (34)$$

which is a  $3.4\sigma$  detection of deceleration between the above two redshifts (though this does assume an external WMAP7 curvature constraint, which introduces some slight level of GR-dependence). However, the desirable goal of verifying that  $z_{\text{acc}} < 1$  as expected is considerably more challenging, since the expected change in  $\dot{a}$  between  $z = 0.67$  and 1 is only 1.7 percent in our default model. The *Euclid* spacecraft (Laureijs et al 2011) is predicted to get sub-percent measurements of  $r_s H(z)$  at a range of redshifts  $0.9 < z < 1.8$ , which looks very promising for a direct model-independent result, while improved ground-based measurements spanning  $0.3 < z < 0.9$  would also be highly desirable.

## 5 CONCLUSIONS

We summarize our conclusions as follows:

(i) The *predicted* value of  $z_{\text{acc}}$  is rather well constrained by current data within  $w$ CDM models, and is mainly sensitive to  $\Omega_m$  rather than  $w$ ; this implies that a direct measurement of  $z_{\text{acc}}$  is not helpful for measuring  $w$ , but is potentially an interesting test of  $w$ CDM versus alternate models such as modified gravity.

(ii) Contrary to intuition, the (probable) downturn in SN residuals relative to the empty Milne model does *not* provide convincing evidence for deceleration. The predicted downturn is strongly dominated by the negative space curvature in the Milne model, and the actual deceleration in  $\Lambda$ CDM makes only a small minority contribution to the downturn.

(iii) There are many advantages to presenting SNe distance residuals relative to a flat coasting model ( $\Omega_m = 0$ ,  $\Omega_{DE} = 1$ ,  $w = -1/3$ ), and also in changing the horizontal axis from  $z$  to  $u = \ln(1+z)$  as in Fig. 4. This presentation enables a number of robust non-parametric deductions about expansion history based on the *global shape* of the observed residuals  $y_D(u)$ , without needing specific numerical derivatives of data or fitting functions. Notably, a turnover in this plot is decisive evidence for deceleration, while any negative curvature in the data points is evidence for higher  $q$  in the past.

(iv) If a turning point in  $y_D(u)$  is observed, then we can infer  $z_{\text{acc}}$  from its location and  $(1+z_{\text{acc}})/E(z_{\text{acc}})$  from its height from Eqs. (31,32); the latter relation holds to very good accuracy in the case of  $w$ CDM models, slightly degrading in the case of large negative  $w_a$ .

(v) For the case of  $w$ CDM models near the concordance range, the model curves of  $y_D(u)$  are remarkably close to simple quadratics to an rms accuracy  $\lesssim 0.3$  percent, significantly better than present data. This provides a simple intuitive visual test for potential deviations from  $w$ CDM.

(vi) For constraining expansion history, there are significant complementarities between SNe and BAO (or cos-

mic chronometers): the SNe have a precise local anchor at  $z \leq 0.05$  and therefore place strong constraints on the *integrated* acceleration, e.g. giving robust lower bounds on the value of  $1.7/E(0.7) \geq 1.1$ . However, the combination of the integral in SNe distances and the broad maximum in  $(1+z)/E(z)$  around the acceleration transition implies that SNe are weak at giving model-independent constraints on  $z_{\text{acc}}$ . In contrast, BAOs offer direct access to  $H(z)$  without differentiation and are therefore potentially stronger at constraining  $z_{\text{acc}}$ ; but they have limited precision due to cosmic variance at  $z \lesssim 0.25$ , and they are therefore weaker at constraining the total integrated acceleration, most of which occurs at  $0 < z < 0.3$ .

It is clearly important to get a good cross-anchor between SN measurements and BAO measurements for constraining the absolute distance scale; as argued by e.g. Sutherland (2012), precision measurements of *both* SNe and BAO at matched redshifts would be very useful for this; see also Blake et al (2011) for a slightly different but related approach.

## ACKNOWLEDGEMENTS

We thank the anonymous referee for helpful comments which have improved the clarity of this paper.

This is a pre-copyedited, author-produced version of an article accepted for publication in MNRAS. The version of record is available online, at Digital Object Identifier DOI:10.1093/mnras/stu2369 .

## REFERENCES

- Anderson L., Aubourg E., Bailey S. et al, 2014, MNRAS, 441, 24.
- Balbi A., Ade P., Bock J. et al, 2000, ApJ, 545, L1.
- Betoule M., Kessler R., Guy J. et al, 2014, A&A, 568, A22.
- Blake C., Glazebrook K., Davis T. et al, 2011, MNRAS, 418, 1725.
- Bolotin Y.L., Lemets O.A., Yerokhin D.A., 2012, Phys. Uspekhi, 55, 9 (arXiv:1108.0203)
- Busca N.G., Delubac T., Rich J. et al, 2013, A&A, 552, 96.
- Cattoen C., Visser M., 2008, Phys. Rev. D, 78, 063501.
- Celerier M.-N., 2007, New Adv. Phys. 1, 29.
- Clarkson C., Zunckel C., 2010, Phys. Rev. Lett, 104, 211301.
- Clifton T., Ferreira P.G., Padilla A., Skordis C., 2012, Phys. Rep., 513, 1
- Cunha J.V., Lima J.A.S., 2008, MNRAS, 390, 210.
- de Bernardis P., Ade P.A.R., Bock J.J. et al, 2000, Nature, 404, 955.
- Efstathiou G., Sutherland W., Maddox S., 1990, Nature, 348, 705.
- Ferrarese L., Freedman W.L., Hill R.J. et al, 1996, ApJ, 464, 568.
- Goobar A., Leibundgut B., 2011, Ann. Rev. Nucl. Part. Sci., 61, 251.
- Hinshaw G., Larson D., Komatsu E. et al, 2013, ApJS, 208, 19.
- Laureijs, R. et al, 2011, Euclid Red Book, arXiv:1110.3193
- Leibundgut, B., 2001, ARA&A, 39, 67.
- Linder E., 2010, Phys. Rev. D, 82, 063514.
- Mortsell E., Clarkson C., 2009, J. Cosmol. Astropart. Phys., 01, 044.
- Mosher J., Guy J., Kessler R. et al, 2014, ApJ, 793, 16.
- Nesseris S., Garcia-Bellido J., 2013, Phys. Rev. D, 88, 063521.
- Peacock, J.A., Cole S., Norberg P. et al, 2001, Nature, 410, 169.
- Percival W.J., Sutherland W., Peacock J.A. et al, 2002, MNRAS, 337, 1068.
- Perlmutter S., Aldering G., Goldhaber G. et al, 1999, ApJ, 517, 565.
- Planck Collaboration XVI, 2014, A&A, 571, A16.
- Riess A.G., Fillipenko A.V., Challis P. et al, 1998, AJ, 116, 1009.
- Riess A.G., Strolger L.-G., Tonry J. et al, 2004, ApJ, 667, 665. (R04)
- Sahni V., Starobinsky A., 2006, Int. J. Mod. Phys. D, 15, 2105.
- Santos B., Carvalho J.C., Alcaniz J.S., 2011, Astropart. Phys., 35, 17.
- Seikel M., Schwarz D.J., 2008, J. Cosmol. Astropart. Phys., 02, 007.
- Shapiro C., Turner M.S., 2006, ApJ, 649, 563.
- Sutherland W., 2012, MNRAS, 426, 1280.
- Suzuki N., Rubin D., Lidman C. et al, 2012, ApJ, 746, 85.
- Turner M., Riess A., 2002, ApJ, 569, 18.
- White S.D.M., Navarro J.F., Evrard A.E., Frenk C.S., 1993, Nature, 366, 429.

## APPENDIX A: PREVIOUS CLAIMS OF DECELERATION

Here, we provide a short discussion of previous claims concerning evidence of past deceleration from SN data; these are mostly in press releases or the semi-popular literature, but have had a significant influence. One of the earliest such claims appears to be a quote from A. Riess on NBC News<sup>3</sup>, 2001 April 02, ‘the new supernova, dubbed SN 1997ff, confirms that the universe began speeding up relatively recently’. A notable Scientific American article (Feb. 2004) by Riess & Turner includes the quote ‘the observations (six SNe > 7 Gyr old) confirmed the existence of an early slowdown period.’ This appears to be partly based on Turner & Riess (2002), and that paper fits two classes of model: first  $w$ CDM models (in which case deceleration occurs almost ‘by assumption’ for reasonable values of  $\Omega_m$ ); and secondly a two-parameter model in which  $q(z)$  follows a step transition between two constant values, an early value  $q_2$  to a late-time value  $q_1$ ; also the transition redshift was artificially fixed at  $z = 0.4$  or  $0.6$ , so this model set is quite restrictive and not very representative of plausible dark energy evolution. Also, the title of Riess et al (2004) (R04) contains the phrase ‘Evidence for past deceleration...’; that paper is (as of 2014) the most-cited astrophysics paper published in 2004, and has thus been highly influential. Specifically, R04 Section 4.1 considers a two-parameter model  $q(z) = q_0 + z(dq/dz)$  with constant  $dq/dz$ , and find that  $dq/dz$  is positive (implying past deceleration) at above the 95% confidence level. Converting to  $z_{acc} = -q_0/(dq/dz)$ , R04 derived  $z_{acc} = 0.46 \pm 0.13$ . However, we note that there are several possible caveats in this result: firstly a constant  $dq/dz$  model is somewhat unphysical since it leads to divergent  $q$  at large  $z$ ; more realistic models like  $\Lambda$ CDM have  $dq/dz$  decreasing with  $z$ , so a linear  $q(z)$  model tends to underestimate  $z_{acc}$ ; a linear  $q(a)$  relation as in Section 3.4, Cunha & Lima (2008) and Santos et al (2011) is probably more realistic. Secondly, the choice of uniform priors in  $q_0, dq/dz$  leads to a prior density which is steeply rising towards small  $z_{acc}$ . If the true model is close to  $\Lambda$ CDM, both of these effects may tend to pull the  $z_{acc}$  estimate low. Thirdly, as seen in Cunha & Lima (2008), inclusion of more recent SNLS SN data also shifts the likelihood contours slightly towards smaller  $dq/dz$ ; most of their samples exhibit some non-decelerating regions inside the 95% confidence contour.

From our discussions above, it appears that there has been a tendency to overstate the strength of evidence for actual past deceleration in SN data; the results of R04, Cunha & Lima (2008), Mortsell & Clarkson (2009) and this paper agree that there is reasonable evidence ( $\sim 2\sigma$ ) that  $q(z)$  was less negative in the past than today, but the GR-independent evidence for an actual zero-crossing (i.e. transition to deceleration) is relatively weak, and sensitive to the choice of parametric form for  $q(z)$ . Thus improved data is highly desirable to prove past deceleration at high confidence.

<sup>3</sup> <http://nbcnews.com/id/3077854>

## APPENDIX B: A SIMPLE APPROXIMATION FOR $D_L$

Here, we note that we can also use the fitting function equation (27) to obtain a simple ‘computer-free’ approximation to  $D_L(z)$  for constant- $w$   $w$ CDM models near the concordance model, which is remarkably accurate up to  $z < 1.7$ . The procedure goes as follows:

(i) For given  $\Omega_m, w$ , the standard Friedmann equation gives the value of  $z_{\text{acc}}$  as in equation (1), hence  $(1 + z_{\text{acc}})/E(z_{\text{acc}})$  follows.

(ii) Given those two values above, we can then readily solve for the pair  $(b_1, b_2)$  in equation (27) which reproduce the same position and value of the turning point in  $(1 + z)/E(z)$ ; the result is  $b_1 = 2[(1 + z_{\text{acc}})/E(z_{\text{acc}}) - 1]/u_{\text{acc}}$ ,  $b_2 = b_1/2u_{\text{acc}}$  where  $u_{\text{acc}} \equiv \ln(1 + z_{\text{acc}})$ .

(iii) Finally inserting the above constants  $b_1, b_2$  in equation (30) gives our simplified approximation for  $D_L$ .

Since this procedure matches only the turning point in  $(1 + z)/E(z)$ , as expected it results in slightly different values of  $b_1, b_2$  compared to the previous case in § 3.3 where we numerically fitted  $b_1, b_2$  to the Friedmann  $(1 + z)/E(z)$  function over the full range  $0 < u < 1$ . Thus we get a less accurate approximation to  $D_L$ , but the accuracy still turns out surprisingly good for this back-of-envelope level approximation. For the case of the concordance model  $\Omega_m = 0.30$ ,  $w = -1$ , the recipe above gives  $b_1 = 0.5960$ ,  $b_2 = 0.5804$ , hence the approximation becomes

$$D_L(z) \simeq (c/H_0)(1 + z)(u + 0.298 u^2 - 0.1935 u^3) ; \quad (\text{B1})$$

comparing this to the quasi-exact numerical  $D_L$  gives an rms error of 0.14 percent and a worst-case error 0.32 percent across the range  $0 < u < 1$  ( $z < 1.72$ ). The accuracy improves for  $w > -1$  and degrades for  $w < -1$ , but remains  $< 0.3$  percent rms across the preferred ranges  $0.27 < \Omega_m < 0.33$ ,  $-1.2 < w < -0.8$ . The recipe above is substantially more accurate than a traditional third-order Taylor expansion in  $z$ , which rapidly becomes poor at  $z > 1$ .

## APPENDIX C: RELATION BETWEEN $q$ AND JERK

Here, we provide a short argument why the simple fitting function of equation (27) works surprisingly well at  $u < 1$ . With the deceleration parameter  $q$  defined as above, and the dimensionless jerk parameter  $j$  defined by

$$j \equiv \frac{d^3 a / dt^3}{a H^3(a)} , \quad (\text{C1})$$

it is shown by e.g. Bolotin et al (2012) that

$$\begin{aligned} \frac{dq}{du} &= j - q(2q + 1) \\ &= \frac{1}{8} + j - 2 \left( q + \frac{1}{4} \right)^2 \end{aligned} \quad (\text{C2})$$

(which is model-independent, assuming only that the derivatives exist). In  $\Lambda$ CDM models,  $j = +1$  independent of time (for negligible radiation content); this implies that  $dq/du$  had a maximum when  $q = -1/4$ , and was slowly varying between  $7/8$  and  $9/8$  over the period with  $-0.60 < q < +0.10$ ,

which corresponds to  $z < 0.86$  and  $u < 0.62$  in our default model. Also, differentiating equation (17) gives

$$\frac{dq}{du} = -\frac{d^2}{du^2} \ln \left( \frac{1 + z}{E(z)} \right) ; \quad (\text{C3})$$

thus a slowly-varying  $dq/du$  leads to near-quadratic dependence for  $(1 + z)/E(z)$  versus  $u$ . We note that this is partly coincidental for parameters near the concordance model, since the present-day value  $q_0 \simeq -0.55$  is near the end of the timespan when  $+0.1 > q > -0.6$ .

This paper has been typeset from a  $\text{\TeX}/\text{\LaTeX}$  file prepared by the author.